ARTICLES

Determination of the gravitational constant with a lake experiment: New constraints for non-Newtonian gravity

B. Hubler, A. Cornaz, and W. Kündig
Physik-Institut, Universität Zürich, 8057 Zürich, Switzerland
(Received 26 October 1994)

The gravitational constant G has been determined at two effective interaction distances 88 m and 112 m, respectively. The $1/r^2$ dependence of the Newtonian gravitational force law is tested by comparing these results with the currently accepted laboratory determination of G. A high-precision balance was used to measure the weight difference of two 1-kg stainless steel masses as a function of the variable water level of a pumped-storage lake. Water-level changes up to 44 m produced a maximum weight difference of 1390 μg, which could be measured with a resolution of 0.5 μg. The difference measurement was carried out to diminish several systematic effects; e.g., tides and balance drifts become negligible. Basically, the measurement directly yields the gravitational interaction between the test masses and the locally moved mass (water and air). Data of weight difference and water level were recorded over several months of the last three years. They yield values for G of $(6.669 \pm 0.005) \times 10^{-11}$ m^3 kg^{-1} s^{-2} at 112 m and $(6.678 \pm 0.007) \times 10^{-11}$ m^3 kg^{-1} s^{-2} at 88 m, both in agreement with laboratory determinations. New constraints on the strength and range of a composition-independent fifth force are set.

PACS number(s): 04.80.Cc

I. INTRODUCTION

The question whether new fundamental intermediate-range forces ("fifth force") exist has been of theoretical and experimental interest for many years [1]. Although the strength was expected to be comparable to gravity, there is as yet no conclusive evidence for such a force. In the meantime the interest has faded away, and the strength of possible new forces, if they exist at all, is supposed to be outside the present experimental reach. A new interaction is usually expressed in terms of a Yukawa potential superimposed on the Newtonian gravitational potential by

$$V(r) = -G_\infty \frac{m_1 m_2}{r}(1 + \alpha e^{-r/\lambda}), \tag{1}$$

where α is the strength of the new force relative to gravity, λ the range of the new force, and G_∞ the Newtonian gravitational constant for $r \to \infty$. The strength can be written as

$$\alpha = \pm \frac{g^2}{4\pi G_\infty}\left(\frac{q_1}{m_1}\right)\left(\frac{q_2}{m_2}\right), \tag{2}$$

where g is the coupling constant and the $+$ and $-$ signs refer to scalar and vector interactions, respectively. *A priori* the coupling charge q is of unknown nature. Constraints on the strength and length of a composition-dependent interaction, which couples to the baryon and lepton number or a mixture of them, are obtained by torsion-balance experiments carried out by Adelberger *et al.* [2] and others.

Assuming that the interaction couples exactly to mass or only slightly to atomic or nuclear structure, experiments searching for distance-dependent deviations of Newtonian gravity are necessary; nevertheless, they are sensitive to any interaction mediated by particles with nonvanishing mass. In this case, the force between two point masses is

$$F(r) = G(r)\frac{m_1 m_2}{r^2}, \tag{3}$$

$$G(r) = G_\infty[1 + \alpha(1 + r/\lambda)e^{-r/\lambda}], \tag{4}$$

and the gravitational "constant" becomes distance dependent.

At astronomical distances no value of G can be provided because of the unknown masses. Instead of it, Newton's law can be tested with high accuracy. The best tests are obtained at the interaction range of 10^{11} m from observations of the perihelion precession for Mercury and Mars [3]. Somewhat less stringent is the comparison of the effective values of $GM_\odot$ for different planets via Kepler's third law. In the range between 10^4 m and 10^9 m the inverse-square law has been confirmed from a comparison of Earth-surface data with the orbital parameters of the Laser Geodynamics Satellite (LAGEOS) and of the Moon, respectively [4].

At laboratory distances (1 cm to 1 m) the best results come from torsion-balance experiments [5] and from a null test performed by Moody and Paik [6] by testing Gauss's law for the gravitational field with a three-axis superconducting gravity gradiometer. Schurr [7] has not

found any deviation of Newton's law by using a Fabry-Pérot microwave resonator as a pair of pendulums in the field of a periodically moved mass.

At geophysical distances (10 m to 10 km), in which our experiment belongs, the less stringent constraints of non-Newtonian gravity are set. With so-called "Airy-type" experiments the gravity gradient towards the center of the Earth is measured by using gravimeters. High tower experiments [8] have put limits on the variation of G with distance, but provide no direct estimate of G itself. In mines [9], in boreholes [10], and in the ocean [11], the value of G could be determined with the density of the traversed material. However, such experiments suffer from the insufficient knowledge of local topography and from density anomalies in the Earth's crust. Additionally, the measurements are disturbed by moving the gravimeters between readings.

Many of these problems can be solved by using movable sources of known mass and fixed instruments. In "lake" experiments the gravity as a function of a variable water mass is measured by using gravimeters and balances in fixed positions. With gravimeters problems result from calibration of instruments and from instrumental drift [12,13]. With a single balance, these problems can be removed. Moore *et al.* [14] employed an electrostatic beam balance in a tower of the Splityard Creek reservoir in Australia. The test masses to be weighed were separated by 12 m yielding an effective interaction distance of 22 m. Their value of G agrees with the laboratory value by $(0.2 \pm 0.8)\%$. The uncertainty was mainly due to vibration of the supporting tower.

In this paper we give a more detailed account of the Gigerwald-lake measurement of the gravitational constant which was determined at an effective interaction distance of 112 m by using an electromagnetic balance [15]. A new result has recently been obtained at an effective interaction distance of 88 m. To distinguish we will refer to these two experiments as the 112-m and 88-m experiment, respectively. Together with the currently accepted laboratory value our results of G improve the existing upper limits of the strength of a composition-independent fifth force in the range between 5 cm to 100 m.

II. THE GIGERWALD EXPERIMENT

A. General principle

The experiment is mounted in the dam of the Gigerwald lake, where a balance alternately measures the weights of two 1-kg test masses located above and below the variable water level of the lake. If the lake were infinite, a plane sheet of thickness $h = 40$ m and density $\rho = 1000\ \mathrm{kg\,m^{-3}}$ would generate, in the case of purely Newtonian gravity, a gravitational field of $2\pi G\rho h \approx 1677\,\mu\mathrm{Gal}$ ($1\,\mu\mathrm{Gal} = 10^{-8}\,\mathrm{m\,s^{-2}}$). This would change the "weight" of a 1-kg test mass by about 1.7 mg. With one test mass located above and one below the water sheet, the total weight difference of these two sites then is $4\pi G\rho h$, or $3354\,\mu$Gal. Placing the test masses in the dam of a finite lake reduces the signal by somewhat more than a factor of 2. It also makes the weight signal more sensitive to the shape of the lake close to the test masses. However, the dam contour of the Gigerwald lake is well defined and can accurately be surveyed. If the weight is measured with a resolution of about $1\,\mu$g and the uncertainties of the lake geometry are small enough, a value of G with an uncertainty of less than 0.1 % should be obtainable.

At a water level h, the gravitational forces acting on the test masses $i = 1, 2$ are

$$\vec{F}_i(h) = \vec{F}_i^{\mathrm{lake}}(h) + \vec{F}_i^{\mathrm{Earth}} + \vec{F}^{\mathrm{tides}}, \tag{5}$$

as is shown in Fig. 1. Since several systematic effects vanish by difference measurements, we have distinguished three sources of gravitational forces: $F_i^{\mathrm{lake}}(h)$ is the force from the water mass of the lake depending on the water level, F_i^{Earth} is the net force from the Earth including inertial forces, and F^{tides} is the net force from extraterrestrial sources (Sun and Moon).

A balance naturally is sensitive to *vertical* forces, where the vertical direction (z direction) is defined by the plumb line. Deviations from this line caused by variations of local gravity are of order 10^{-6} and are not detectable by the balance. Since a single balance is used, several systematic effects can be eliminated by measuring the weight difference $\Delta F^z(h) = F_1^z(h) - F_2^z(h)$ in a short time (about 13 min in our case). Any forces which act nearly identically on both test masses are not observed. Hence, gravitational forces from extraterrestrial sources and from the farther environment of the lake are not critical and can-

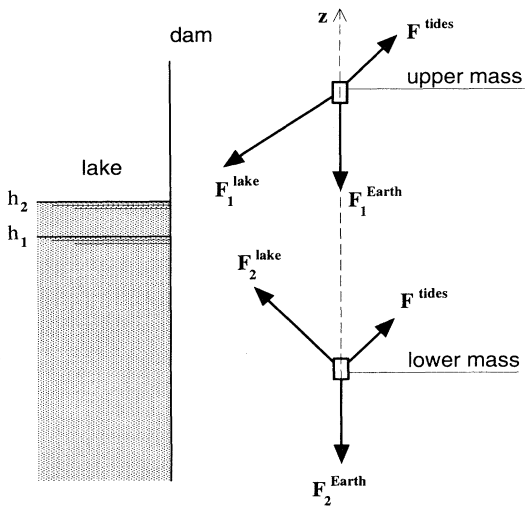

FIG. 1. Forces on the upper and lower test mass. The magnitude of the plotted forces are not true to scale. If F_1 and F_2 are the weight forces on the two test masses 1 and 2, the double difference measurement $[F_1^z(h1) - F_2^z(h_1)] - [F_1^z(h_2) - F_2^z(h_2)]$ at two water levels h_1 and h_2 yields the gravitational interaction between the locally moved mass (water and air) and the test masses.

cel out by the difference measurement. Basically, for a point source at a large distance r from the test masses, $\Delta F^z(h)$ decreases independent of the angle of direction with d/r^3, where d is the test mass separation. In the same way, a slow balance drift vanishes by the difference measurement, which may arise from variable stresses inside the balance or from a slow thermal drift.

Gravity is increasing by about 300 μGal m^{-1} towards the center of the Earth. By measuring the difference $\Delta F^z(h_1) - \Delta F^z(h_2)$ at two different water levels, h_1 and h_2, respectively, even the resulting difference of local gravity at the upper and the lower mass vanishes. Indeed, the gravity difference (due to the Earth) must be constant in time with respect to the measuring period. Local tidal effects and displacements of the ground caused by loading and unloading it by moving water may cause a slight variation of local gravity. However, because the test masses are moved in the same way, the changes in first order have the same magnitude and become negligible. Finally, the interaction between the locally moved mass (water and air) and the test masses is observed directly.

B. Experimental setup

The experimental site is at the Gigerwald lake, which is a pumped-storage reservoir for peak-power production in a narrow valley of eastern Switzerland (46°55′ N, 9°24′ E at 1335 m above sea level). The lake is about 2.5 km long and about 400 m wide. The utilizable capacity is 33.4×10^6 m^3. A 147-m-high concrete dam of parabolic shape confines the lake downstream allowing maximum water-level changes of 90 m. Except on weekends water is released during the day with a maximum drain rate of 74 m^3 s^{-1}. The pressure line leads to the power plant at an altitude of 850 m, seven kilometers away. During the night water is pumped back from the corresponding reservoir with a maximum pump rate of 36 m^3 s^{-1}. Normally, daily water-level changes are less than 3 m depending on power consumption and water afflux. At the beginning of spring the water level is lowered to accommodate the melting snow.

A cross-sectional view of the dam is shown in Fig. 2. The balance, the electronics, and the data-acquisition computer were set up in a small, thermally isolated room at the top of the central plump shaft of the dam, which is used by the power company for controlling dam movements. The room is reached through a small access from the transverse gallery 6 m above. The vertical shaft is 1 m in diameter and 108 m long. The test masses are hung from the balance by tungsten wires, one at the top of the shaft immediately below the balance and one at the bottom of the shaft. The balance itself is placed on a massive granite plate supported by a pair of thick aluminum girders. Additionally, the plate is damped by three cork buffers. It protects the balance from ground vibrations, which in fact have never been observed (except for earthquakes).

To avoid air convection and variable buoyancy the balance and the two test masses are held in vacuum (at about 10^{-3} mbar). To this end a 10-cm-diam vacuum tube of stainless steel consisting of 3-m-long pieces was employed. It is freely hanging on a second pair of aluminum girders at the top of the shaft and is guided only with loose tube clamps. The vacuum connection to the vessel with the balance in it is established by metal bellows to avoid propagation of vibrations to the balance. A turbomolecular pump is connected to the tube in a lower gallery.

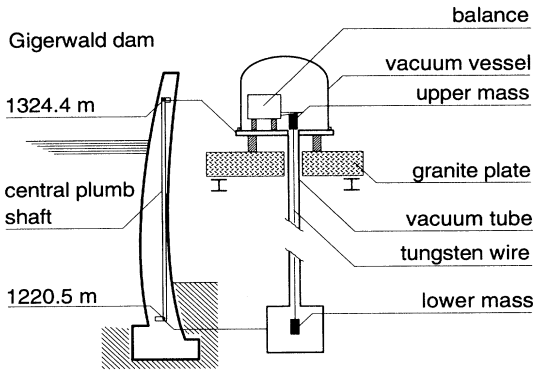

FIG. 2. Cross section of the Gigerwald dam. At the top of the central plumb shaft the balance is installed in a vacuum system consisting of a vessel and a long tube. One mass is suspended immediately below the balance, and the other mass at the bottom of the shaft with a long tungsten wire.

C. Weighing appliance

1. Balance design

The balance used in this experiment is a modified Mettler-Toledo mass comparator. A schematic view is shown in Fig. 3. It is a single-pan flexure-strip balance allowing the comparison of 1-kg masses. It works on the substitutional principle, which means that the masses to be compared are placed one after the other on the

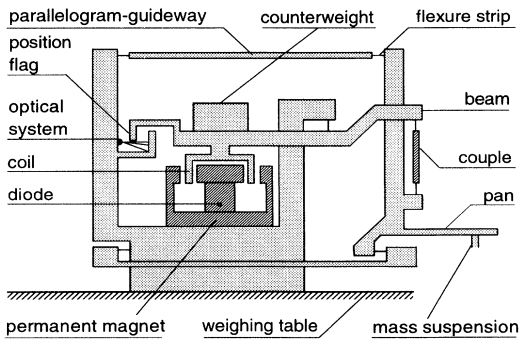

FIG. 3. Schematic side view of the flexure-strip balance.

same pan. To eliminate unfavorable torques the pan is fixed to a parallelogram guideway, with which horizontal forces are transmitted to the massive support of the balance. The guideway is suspended by 100-μm-thick flexure strips, and the suspension pan, where the weights are attached, moves in the vertical direction with practically no friction. The vertical forces are transmitted on the balance beam via a couple, which consists of two vertical thinned flexure strips rotated to each other by 90°. The beam itself is suspended by two flexure strips defining a sharp nonmovable pivot.

The weight of an attached mass is mainly compensated by a fixed counterweight. Up to 2 g are electrically compensated by a current through a coil in the field of a permanent magnet. This current is governed by a control loop to maintain the beam in a horizontal position. The beam position is monitored by an optical detector. The magnitude of the measured coil current is used as a gauge of the weight of the attached mass.

Because the balance is never arrested (the load on the beam is held constant within 1 g during the mass exchange, see Sec. II C 5), the mechanical components of the balance are only slightly moving. This avoids relaxation effects in the flexure strips and leads to a very significant improvement in reproducibility of the balance. Together with a good thermal stabilization (Sec. II C 4), it enabled us to make comparisons of 1-kg masses with a stability of about 0.5 μg over one day.

2. *Test masses and suspension wires*

The two test masses were machined of stainless steel 316L and trimmed by grinding down the edges. Afterwards they were finely polished and weighed. Their masses were determined with an accuracy of better than 10 mg with a Mettler PM2000MC. The upper mass of 1.114 45 kg is a hollow cylinder with a height of 4.99 cm and an inner and outer radius of 1.25 cm and 3.25 cm, respectively. The lower mass of 1.098 87 kg is of cylindrical shape, with a height of 5.87 cm and a radius of 2.75 cm. Additionally, the latter has a small cone with a rounded apex in the middle of the bottom side (see Fig. 4). The test masses are equipped with small hooks of stainless steel, which were attached to the masses by cold pressing (two hooks for the upper and one hook for the lower mass, respectively). Screw holes are avoided considering bulk diffusion or absorption, which is not well quantified in vacuum.

The suspension wires are of 0.1-mm-diam tungsten. They were crimped at the ends with small tubes of stainless steel forming small loops in which the test masses are hooked. The wire of the lower mass was attached to a suspension device with a crimped small tube fitted in a slot to define a sharp pendulum pivot. After evacuation the long suspension wire was annealed. Its mass (including crimped small tube) was determined with the balance to be 15.72 g for the 112-m experiment and 9.58 g for the 88-m experiment. For the 112-m experiment an additional mass of 1.00 g was placed on the lower mass to equalize the weights of two test masses (taking into account the masses of the suspension devices). For the 88-m experiment it was replaced by a mass of 7.00 g.

The test mass positions were determined with conventional surveying techniques. On the basis of the regularly surveyed traverse stations inside the dam [16], several reference stations (fixed bolts) were surveyed at the top and at the bottom of the plumb shaft. The average uncertainty of the test mass positions is about 3 mm (with respect to the local coordinate frame). The absolute altitude of the center of mass was determined to be 1324.359(1) m for the upper mass and 1220.537(1) m for the lower mass, respectively, yielding a separation of 103.822 m for the 112-m experiment. In the 88-m experiment the distance between the test masses was shortened by positioning the lower mass upwards to an altitude of 1261.091(1) m yielding a separation of 63.268 m.

3. *Mass suspensions*

The weight of the suspension devices are of 4.24 g and of 3.04 g for the upper and the lower mass, respectively. Each of them consists of three elements: right at the bottom there is a suspension-wire link, in the middle a chain-link-like gimbal where the masses are coupled to the balance, and at the top a double-coned gimbal where the masses are lifted from the balance (see Fig. 4).

The aim in designing the mass suspensions is to minimize unwanted torques on the balance beam, which for

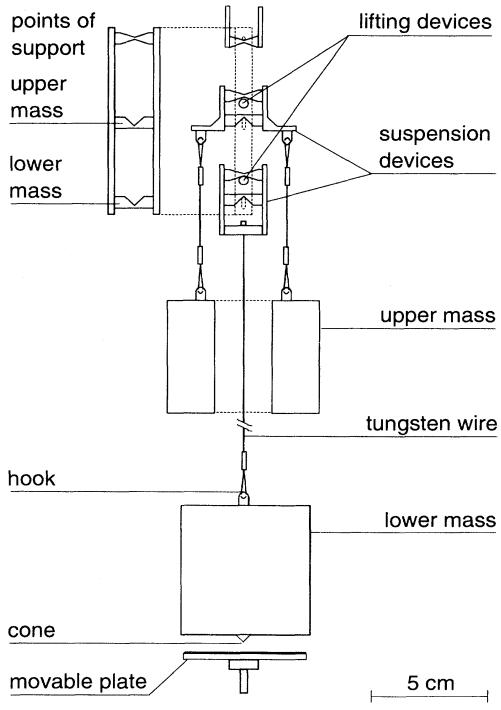

FIG. 4. Schematic side view of the test masses and suspension devices.

example may arise from nonreproducible placings of the masses. This means, the center of gravity of the suspended masses (suspension plus load) should lie on the same vertical axis below the pan when the masses are connected to the balance. This is achieved by a novel designed chain-link-like gimbal made of stainless steel with a saddle surface in the middle. The curvatures at the saddle point are of 0.25 mm in one direction and 0.50 mm perpendicular to it. The surfaces are well polished and coated with layers of tungsten carbide and carbon WC/C (in all about 5 μm). The low friction coefficient and the lamellar coating avoid microwelding. WC/C is a solid lubricant, nevertheless very hard, and the roughness of the surface becomes even smaller with time; in spite of this it is well resistant against abrasion. Because of its low friction coefficient the displacement of the bearing point out of its centering position is estimated to be $< 50\,\mu$m. This well-defined placement also limits the double-coned lifting devices in their position; and vice versa, the same lifting leads to the same equilibrium position of the bearing point when the mass is suspended anew.

On the other hand, torques may be due to mass swings, driven by shocks when raising or lowering a mass during the mass exchange. Oscillations of the upper mass were never seen. The lower mass, however, can be excited to different oscillation modes. The suspension wire causes a vertical spring oscillation with $T_S \approx 1.3$ sec. This mode is damped by the electronic control loop of the balance (at 0.1 Hz). Pendulum oscillation ($T_P \approx 20.4$ sec) gives rise to a centrifugal force. A deflection of $\delta x = 1$ mm would increase the weight by $\delta m = m(\delta x)^2/l^2 \sim 0.1\,\mu$g, where l is the length of the suspension wire. This weight oscillation is beyond the resolution of the balance. A deflection could not be observed. Pendulum oscillations as well as torsional oscillations ($T_T \approx 19$ min) are removed by means of a movable plate covered with elastic plastic foam touching the small cone of the lower mass from below when it is not being weighed. The plate is then smoothly removed just before the mass is to be measured.

Below the pan of the balance, two pairs of double-crossed knife edges are placed to further reduce remaining torques (not shown in Fig. 4). They are made of ceramics and hardened steel.

4. *Temperature stability*

In any balance, a comparison between two masses requires that the effective arm lengths of the beam be constant or drift uniformly by a small amount. To achieve an accuracy of 1 part in 10^9 (1 μg for 1-kg masses) the arm length of a 5-cm-long balance beam must not vary more than 0.5 Å between successive readings. Thermal expansion of the beam may also cause sudden relaxation of strains where different materials are joined together. For this reason a three-stage temperature control system is employed.

Inside the dam the temperature varies between 10 °C and 15 °C during a year. The small room where the balance is set up is isolated and held constant within 0.2 K by using a controlled heater. The vessel, which contains

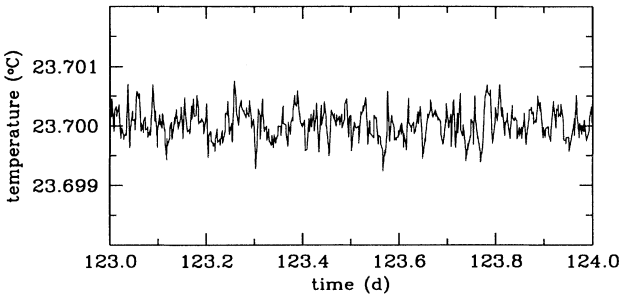

FIG. 5. Temperature stability of the balance during one day.

the balance, and the electronics governing the balance are thermally shielded. This shield consists of copper tubing in good contact with the vessel and a cover of a 3-cm layer of plastic foam insulation. Water is circulated through the copper tubes from a controlled bath with a stability of ± 0.01 K. The balance itself is surrounded with a 2-cm-thick copper case containing a water circulation from a second water bath placed inside the first shield. A gear-wheel pump delivers water, whose temperature is regulated by the computer via a 500-mW heater and a diode-temperature sensor placed at the balance. The proportional integrating-differentiating (PID) control loop with experimentally determined constants yields a long-term stability within 1 mK (see Fig. 5). The random uncertainty is only 0.3 mK.

5. *Weighing procedure and calibration*

The interchange of masses required by the weighing procedure works on a fully automated basis. After a test mass, say the upper mass, is attached to the balance, it is weighed over a period of about 3 min producing an average weighing value. Afterwards it is slowly detached from the balance by slightly lifting it, the other mass is simultaneously lowered and attached to the balance to be weighed in the same way. The mechanism for lifting a mass comprises a vertical double-coned gimbal for each mass, which, on being raised, lifts the mass from the balance by about 1 mm (see Fig. 4). They are moved hydraulically by stepping motor pumps, which are placed outside the vacuum vessel to avoid operating problems in vacuum and to remove variable magnetic fields and disturbing heat sources near the balance. During the mass exchange of about 3 min the weights of the two test masses are controlled by the computer. The load on the balance does not exceed 1 g, and the movement of the balance beam resulting from lifting and lowering the masses is small. A better reproducibility of weight measurements is reached.

Comparing the upper and the lower mass, say A and B, the weighing sequence used is simply

$$\underbrace{A,B}_{1},\underbrace{A,B}_{2},\ldots,\underbrace{A,B}_{60},A+s, \tag{6}$$

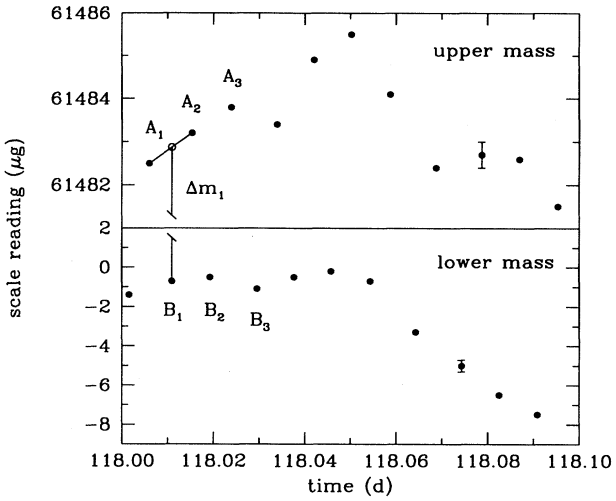

FIG. 6. The two test masses A and B are alternately weighed with a period of about 13 min. The weight difference Δm is simply determined by taking the mean value of two successive measurements of the upper mass at the time the lower mass is measured. Since the weights are compensated by a fixed counterweight, the whole gravity effect is seen in the weight of the lower mass.

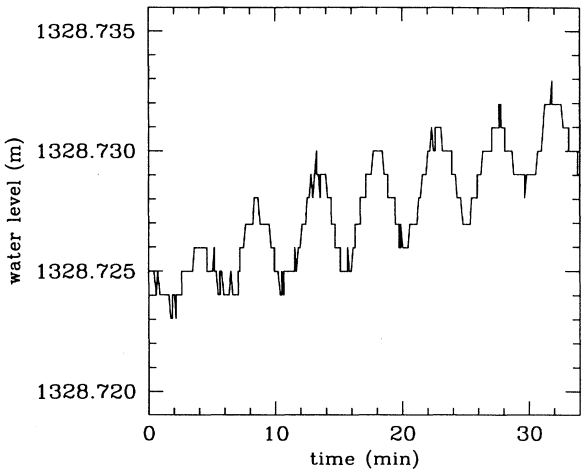

FIG. 7. Water level as a function of time. The low-frequency oscillations ($T \approx 4.7$ min), so-called "seiches," are mainly excited by the wind. The steps mark the digital resolution of the manometer.

where after 60 cycles a calibration of scale sensitivity is carried out by adding a small mass s of 0.999 993 g to the upper mass. No significant change of scale sensitivity was observed (< 1 μg). The effective weights are obtained by multiplying the readings with the value of local gravity at the balance. A gravimeter measurement yielded a value of 9.804 208(3) $\mathrm{m\,s^{-2}}$ [17]. The weight difference is then calculated by linear interpolation between two successive measurements of the upper mass at the time the lower mass was measured (see Fig. 6).

D. Lake survey

1. *Water level*

In the idealized case of an infinite lake, a plain sheet of water with thickness h and density ρ generates a gravitational field independent of the distance from the sheet and proportional to ρh. The proportionality approximately remains true in the case of a finite lake. It is therefore advantageous to determine the water level via hydrostatic water pressure $\rho g h$ instead of floats or similar methods. The pressure measurement automatically corrects in a good approximation any water density variations.

A high-precision manometer (Rittmeyer W1Q) was installed at an altitude of 1240.31 m in a lower gallery of the dam 95 m below the maximum water level. It consists of a quartz resonator whose frequency shift is proportional to the applied absolute pressure. The resolution of the pressure measurement is 10^{-5}, which is less than 1 cm in the water level. The ambient air pressure is measured separately and is subtracted from the total pressure value. Considering water density ρ_W, air density ρ_a, compressibility of water β, as well as local gravity g, the water level h is determined with the formula

$$h = \frac{1 - e^{-\beta P}}{\beta g(\rho_W - \rho_a)}, \tag{7}$$

where P is the measured water pressure.

Calibration of water level was made by precision leveling on several days. An independent calibration was obtained by measuring the altitude of the pressure element and the temperature profile of the lake water. Together with the measured pressure the corresponding water levels could be calculated. Both methods agree with each other and the absolute values of water levels are found to be accurate within 1 cm. Measurements revealing fundamental oscillations of the Gigerwald lake ("seiches") are shown in Fig. 7.

2. *Water density*

The density of the lake water was measured in the laboratory with a pycnometer of the Gay-Lussac type (with an inner volume of 102.845 ml at 20 °C). The water was carefully filled and brought into thermal equilibrium within 0.01 K in a constant-temperature bath at 27.3 °C. To prevent water evaporation, the capillary pycnometer was made airtight with a polyethylene foil. After cooling down to room temperature, the pycnometer was weighed with a Mettler H54AR with an accuracy of 1 mg. The cooling is important to avoid air convection in the balance. Furthermore, water absorption of the pycnometer surface depends on the temperature and humidity of the surrounding air. The pycnometer volume was calibrated with pure water with a relative accuracy of 10^{-5}. By

TABLE I. Water density measurements at 27.3 °C.

Sample I	0.996459 g cm^{-3}
Sample II	0.996468 g cm^{-3}
Sample III	0.996458 g cm^{-3}
Pure water	0.996342 g cm^{-3}

measuring the weight of the empty and filled pycnometer water density was determined for three water samples. Lake water turned out to be slightly denser than pure water by $1.2(2)\times10^{-4}$ g cm^{-3} (see Table I).

Depth profiles of water temperatures were measured on several days down to 80 m by lowering a Pt-100 resistance thermometer. Only very small temperature variations were observed except for a thin layer of about 5 m below the lake surface depending on climatic conditions. Below this boundary layer, temperature usually varies not more than 0.2 K. The annual temperature variation is sinusoidal with extrema in March and September at average temperatures of 3 °C and 10 °C, respectively. During the measuring period water temperature varied from 3 °C to 6 °C. In this range water-density variation is negligible with respect to our required accuracy.

At the lake surface the density is 1.000 09(4) g cm^{-3} corresponding to a mean temperature of 3.5 °C. With a compressibility of 4.9×10^{-10} Pa^{-1} density profiles were computed for all relevant levels. The density which enters the calculation of the weight signal is the density difference between water and air, since water is replaced by air and vice versa, when water level falls or rises. The mean density of air is determined to be 0.001 08(2) g cm^{-3} corresponding to the mean atmospheric pressure at the altitude of 1330 m. The assigned error to it is due to air pressure variations.

3. Lake contour

The lake is situated in a narrow valley and is confined on the sides by massive rock partly covered with scree. Downstream the lake is confined by a smoothly curved concrete dam, which was constructed following simple polynomials. A horizontal section is just a parabola. Fixed pillars spread around the lake are used to establish a local control network. These pillars are regularly controlled by geodetic engineers and are known in position and height within 1 mm in the local coordinate system.

To ensure the exact dam shape a survey of the lakeside was conducted. To this end, more than 100 survey marks were fixed at various locations of the dam when the lake reached its minimum level at the beginning of spring. Subsequently, the marks were surveyed with electronic theodolites (Wild T3000) from the pillars and from free stations. The overestimated data yielded the positions with an accuracy of about 3 mm. They agree with the construction plans within 2 cm.

The shore contour was determined by air photogrammetry. The scan of the lake shore produced survey points at 4-m spacing up to 600 m from the test masses. The obtained random uncertainty of the coordinates is 30 cm.

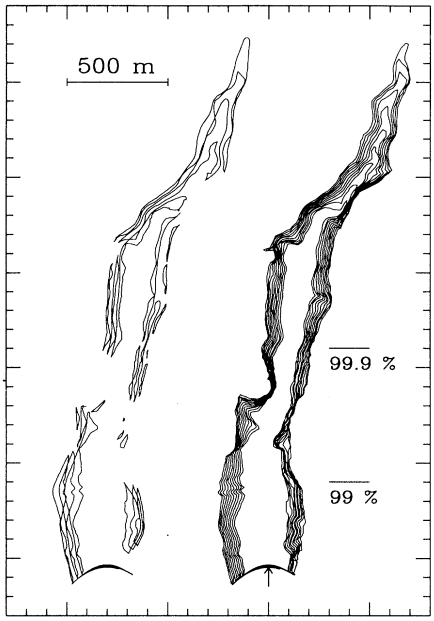

FIG. 8. Contour maps of the Gigerwald lake. Right: Contour lines of the lake shore (6 m equidistant). The arrow marks the position of the balance and the test masses. Left: area of scree (20 m equidistant), displaced sidewards for display purposes. The contribution to the weight signal which originates from the water up to 450 m distance from the dam is already 99%.

The systematic uncertainty is negligible, since the high precision of the pillar coordinates strongly limits any systematic displacement. For larger, noncritical distances an older survey plan of the lake was used which revealed only small deviations from the new plan. Data processing yielded 2-m-equidistant contour lines (see Fig. 8).

4. Scree

The shore is not bounded entirely by rocks. There is also some scree, where water is seeping in. The scree is throughout debris, which is embedded in mud. The porosity of the scree is estimated by geologists to be 0.30 ± 0.03, where the assigned uncertainty is at the 1σ level. This value is quite reasonable considering measurements by other geologists under similar conditions.

From geological surveys based on numerous drill holes the solid rock boundary, and with this the area of scree, is known (see also Fig. 8). Up to 200 m distance from the test masses the amount of scree is negligible. There, the shore is mainly confined by concrete and massive rock. Since 90% of the weight signal comes from the water up to 200 m distance from the test masses, the contribution of water seepage to the weight signal is not negligible though, but small: it is calculated for a mean water level and amounts to 0.6% for the 112-m experiment and 0.4% for the 88-m experiment, respectively.

The scree volume decreases with water level. For the

88-m experiment the scree correction varies between 0.3% and 0.5%. For the 112-m experiment, it is 1.2% at the lowest water levels and decreases for higher levels down to 0.4%. This height dependence offers an internal consistency check for the scree correction. It is proved that the results obtained from data at low water levels are consistent with those obtained at high water levels and support the quoted value for the porosity (see Sec. IV B). Additionally, the value of the 88-m experiment is consistent with the value of the 112-m experiment, where the main scree corrections originate from different regions of the lake.

III. CALCULATIONS

A. Lake integration

To calculate the weight difference as a function of water level the method of Talwani and Ewing [18] is used. In general it is not possible to obtain an analytical expression for the integration of the gravitational force caused by an irregularly shaped three-dimensional body, but the problem is greatly simplified if one of the dimensions becomes infinitesimal. To take advantage of this we divide the three-dimensional body in a large number of thin laminae of thickness dz and add them together. Including a fifth force of the form given in Eq. (1) the vertical gravity caused by an arbitrarily shaped, horizontal lamina can be expressed by contour integrals. The vertical gravitational force dF^z on a mass m located at the point P is (see Fig. 9)

$$dF^z = k\rho\left[\oint d\psi - \oint \frac{z}{r'}\,d\psi\right] dz + \alpha k\rho\left[e^{-|z|/\lambda}\oint d\psi - \oint \frac{z}{r'}e^{-r'/\lambda}d\psi\right] dz, \quad (8)$$

with $k = -G_\infty m$ and ρ the density of the lamina. The contour integral $\oint d\psi$ is 2π, if the vertical projection P' of the point P lies inside the lamina and vanishes otherwise.

Assuming the contour of a lamina may be approximated by a sufficiently large number of discrete points, the first term in Eq. (8) describing Newtonian gravity can be analytically solved [18]. The second term describing the interaction of a fifth force must be numerically integrated. To extract a value for the gravitational constant from data, pure Newtonian gravity is assumed (α=0).

The Gigerwald lake is integrated by using 2-m-equidistant contour lines, each containing 4000 to 5000 individual survey points. The cylindrical test masses are taken as point masses in their centers of mass. The suspension devices and the suspension wires are divided into distributed point masses. The wire of the lower test mass, for example, is divided into 16 point masses equidistantly distributed along the wire axis. The error made by these approximations is far outside the required accuracy of this experiment. The integrated effect for the 88-m experiment and the 112-m experiment, respectively, are shown in Fig. 10. As long as the water level is well between the test masses, the weight difference varies almost linearly with water level as would be expected in the case of an infinite lake. The slope is about 33 μg m^{-1}. Whenever the water level approaches the height of the upper mass (at an altitude of 1324.359 m), the weight signal diminishes and becomes even negative for higher levels. A zero effect would arise for an infinite lake.

The effective interaction distance r_{eff} characterizing the mean distance between the interacting water and the test masses is given by

$$r_{\text{eff}} = \left(\int r_1\,df_1^z - \int r_2\,df_2^z\right) \Big/ \left(\int df_1^z - \int df_2^z\right), \quad (9)$$

where df_i^z is the vertical gravitational force between a water element and the test mass i separated by the distance r_i. The integration over the Gigerwald lake yields $r_{\text{eff}} = (112 \pm 2)$ m and $r_{\text{eff}} = (88 \pm 2)$ m, respectively, slightly depending on water level.

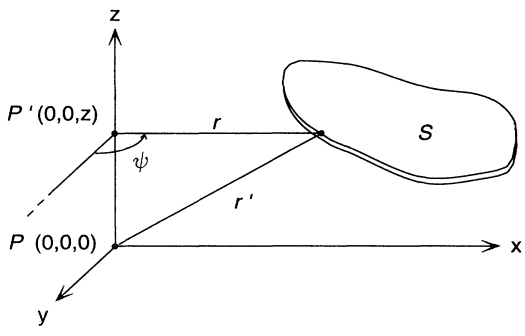

FIG. 9. Geometrical elements involved in the computation of the vertical gravity of a thin horizontal lamina S of constant density. P is the point where the gravity is being evaluated.

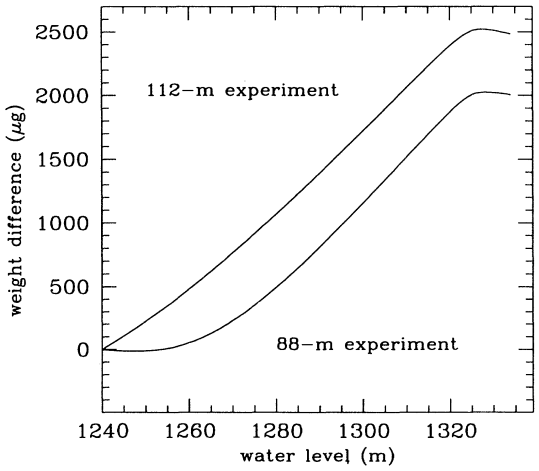

FIG. 10. Calculated weight difference as a function of water level following pure Newtonian gravity. The upper curve is calculated for the 112-m experiment, the lower curve for the 88-m experiment. The origin is set to 1240 m for both curves.

It follows from calculations that the contribution to the weight signal of the lake water situated more than 500 m away is already less than 1%.

B. Systematic uncertainties

In the following the most significant systematic uncertainties listed in Table II are discussed. The largest uncertainties to be expected in the predicted gravity effect are contributions from uncertainties in the geometry of the lake. Since they depend on water level, the magnitude assigned to them are values corresponding to an average water level.

The face of the dam is a smooth surface and is very carefully surveyed within 3 mm. Penetration of water into the concrete is negligibly small. Dam movements, which arise from temperature changes of the dam and from water pressure changes, are continuously registered with several plumb lines. The maximum displacement at the top of the dam is $\pm$ 2 cm corresponding to extreme conditions of an empty lake and a warm dam (contrary to a full lake and a cold dam, respectively). Since in first order both lake water and test masses are moved in the same way, dam movements are not critical. Any balance tilts due to dam movements cancel out by measuring the weight difference and by repeating scale calibration. The final uncertainty of the dam contour is taken to be 1 cm yielding a relative uncertainty contribution of 0.30×10^{-3}.

The shoreline coordinates have an uncertainty of 30 cm. A random perturbation calculation yielded a relative uncertainty of 0.37×10^{-3} for the 112-m experiment. More critical is the seepage of water into the scree. Although the location of solid rock is well known by numerous soil explorations, the porosity of the scree is not well validated and leads to a major contribution in the error budget (see Sec. II D 4). The calculated relative uncertainty for a porosity of 0.30 ± 0.03 is 0.61×10^{-3}. Since these uncertainties scale more or less linearly with the test mass separation, they could be reduced for the 88-m experiment. The calculations yield relative uncertainties of 0.23×10^{-3} for the shore contour and 0.39×10^{-3} for the porosity of scree, respectively.

The test mass positions are not critical. They are determined with electronic theodolites, laser range finders, and leveling instruments referring to the regularly surveyed reference stations inside the dam. The uncertainty in position is found to be about 3 mm. Thermal expansion of the suspension wire is $\pm$ 2 mm at most. The relative uncertainty of test mass positions is about 0.04×10^{-3}.

The water level is known with an accuracy of 1 cm producing a relative uncertainty of 0.12×10^{-3}. Earth curvature was found to be negligible ($<10^{-5}$). Waves average out, and the amplitudes of low-frequency oscillations of the lake ("seiches") are too small to have influence on the weight measurements. The uncertainty of the water density leads to a relative uncertainty of less than 0.05×10^{-3}.

The effect of variable air density is $<0.1\,\mu$g, which is below the resolution of the balance. More problematic is the variable soil moisture in the surroundings of the dam. The effect may vary between $\pm2\,\mu$g depending on climatic conditions. It averages out over a measuring period of some months if it is not correlated with the water level.

The value of g near the balance is easily determined with a relative uncertainty of 10^{-6} by using a gravimeter. It produces an uncertainty of the same magnitude in the error budget.

TABLE II. Contributions to the systematic uncertainty of G in parts per 1000 (1σ).

Source	112-m exp.	88-m exp.
Dam contour	0.30	0.30
Shore contour	0.37	0.23
Porosity of scree	0.61	0.39
Test mass positions	0.04	0.04
Water level	0.12	0.12
Water density	0.05	0.05
Total	0.79	0.56

IV. RESULTS

A. Raw data

The data acquisition is performed on a highly automated level. Measured weights of the test masses and of the calibration mass, water level, balance temperature, vacuum pressure, and climatic conditions are continuously recorded by the computer and displayed as a function of time. Various other system parameters are also registered and can be remote controlled from Zürich. The raw data of the 1994 measurements are shown in Figs. 11 and 12, where the weight difference of the two

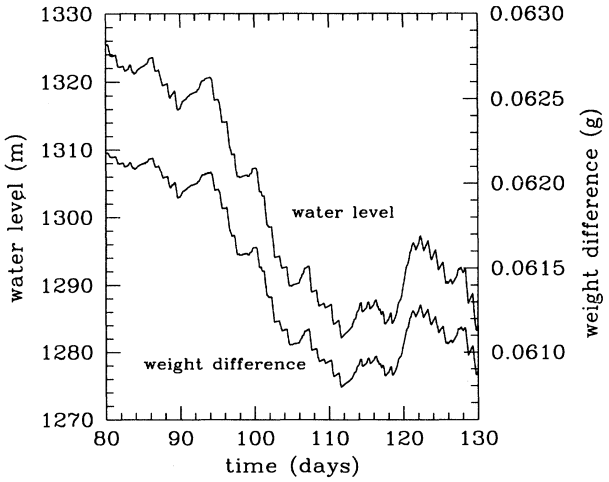

FIG. 11. Water level and weight difference of the 112-m experiment (March to May 1994).

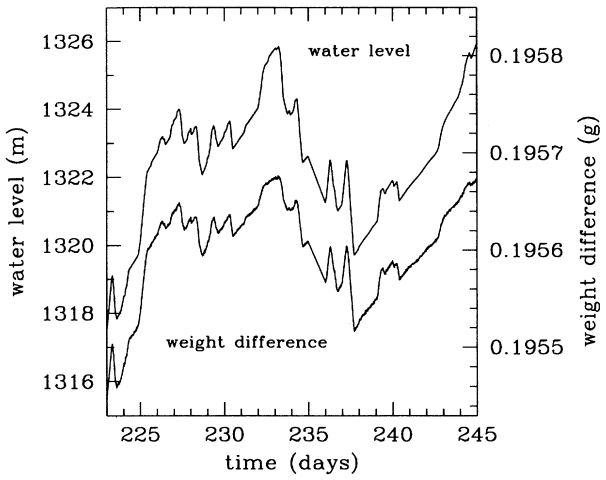

FIG. 12. Water level and weight difference of the 88-m experiment (August 1994).

test masses and the water level are displayed as a function of time. During the spring measurements (over a period of 50 days) water-level changes up to 44 m produced a maximum weight signal of 1390 μg. During the autumn measurements (over a period of 22 days) a maximum weight difference of 223 μg was still obtained.

B. Data analysis

The measured and calculated weight difference (Spring 1994) as a function of water level is shown in Fig. 13.

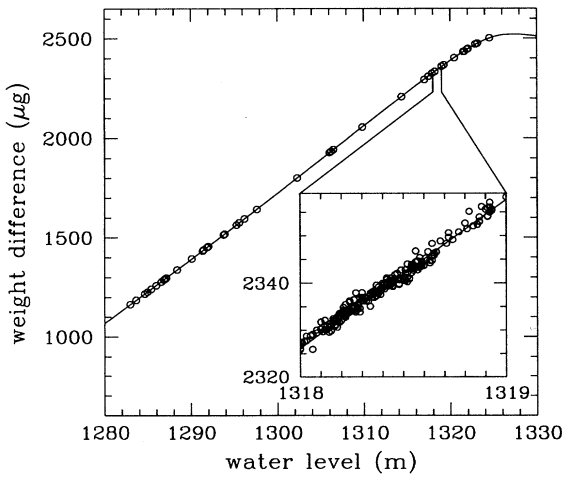

FIG. 13. Weight difference as a function of the water level in Spring 1994 (the origin is set to 1240 m). The measured gravity data (open circles), only corrected for linear drifts, fit well the predicted gravity effect (solid curve). Each circle represents the average of 100 measurements. The insert shows a typical region where all gravity data are presented.

Although an arbitrary balance drift cancels out by the difference measurement, a nonregular and uncorrelated small drift was observed in the weight difference. This drift may originate from changes of soil moisture in the surroundings of the dam. Since the weight-difference data at the same water levels must be equal for all times, any discrepancies arising from such slow drifts could be minimized by using the following model equation for the weight difference:

$$\Delta F(t) = a\Delta F_{\text{Newton}}(t) + b_i t + c_i, \tag{10}$$

where $\Delta F_{\text{Newton}}(t)$ is the calculated weight difference based on Newtonian gravity. The fit parameter a, valid over the whole measuring period, represents the ratio G/G_{lab}, where $G_{\text{lab}} = 6.6726 \times 10^{-11}\,\text{m}^3\,\text{kg}^{-1}\,\text{s}^{-2}$, the currently accepted laboratory determination of the gravitational constant [19], is used as an arbitrary reference. The parameters b_i and c_i, respectively, are coefficients of linear drifts over time intervals between 5 hours and 3 days. The magnitude of b_i is less than 0.5 μg per day and is of variable sign; c_i adjusts the fit to be continuous. The coefficients follow from a regression analysis with the method of least squares. The results for a including the 1992 and 1993 measurements [15] are given in Table III.

For the 112-m experiment, the final value of a is determined to be 0.999 44(17), which is the weighted mean of the 1992, 1993, and 1994 measurements. For a consistency check the 1993 data were subdivided into two data sets of measurements with water level above and below 1305 m. The results are 0.999 29(26) and 0.999 81(33), respectively, in reasonable agreement with each other. They also confirm the calculations made for the scree correction. If the provided value for the porosity were wrong by 20%, the two results should already differ by more than 0.1%, which is not the case. The discrepancy of the 1994 value is assumed to be due to meteorological changes in the immediate environment of the lake (e.g., variable soil moisture), and due to nonreproducible positioning of the test masses on the suspension devices. For the 88-m experiment, the resulting value of a is found to be 1.00079(94). The larger statistical uncertainty of 0.94×10^{-3} is mainly due to the shorter measuring time and the smaller weight signal.

The total uncertainty of G is obtained by taking the root-mean-square of the uncertainties listed in Table II plus the corresponding random experimental uncertainties. The resulting values of the gravitational constant are

$$G = (6.669 \pm 0.005) \times 10^{-11}\,\text{m}^3\,\text{kg}^{-1}\,\text{s}^{-2} \tag{11}$$

TABLE III. Results of the 112-m experiment and the weighted mean.

Data	$a = G/G_{\text{lab}}$
1992	1.00017(76)
1993	0.99958(19)
1994	0.99822(48)
Weighted mean	0.99944(17)

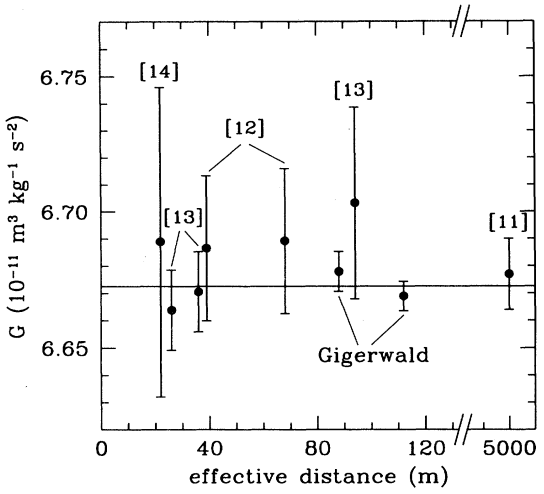

FIG. 14. Results of G experiments at geophysical distances as a function of the effective interaction distance. The solid line represents the laboratory value G_{lab}. Numbers in brackets refer to the reference list.

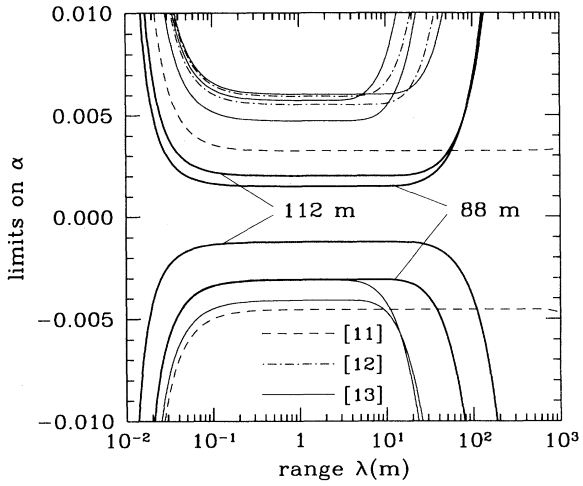

FIG. 15. Constraints for a composition-independent fifth force set by the Gigerwald experiment and by other G experiments at geophysical distances. The strengths α and ranges λ in the area below the curves ($\alpha < 0$) and above the curves ($\alpha > 0$) are excluded with 95% confidence. The numbers in brackets refer to the reference list.

for the 112-m experiment, and

$$G = (6.678 \pm 0.007) \times 10^{-11}\,\mathrm{m^3\,kg^{-1}\,s^{-2}} \qquad (12)$$

for the 88-m experiment. The values are in agreement with each other and with the accepted laboratory value (see Fig. 14).

Together with Luther's laboratory value $G_{\text{lab}}(r_{\text{eff}} \approx 5$ cm) the values of the gravitational constant determined from the Gigerwald experiment place new limits on the strength $\alpha(\lambda)$ of a composition-independent fifth force. With $G(r_2)/G(r_1) = \beta$, the ratio of gravitational constants determined at two different distances r_1 and r_2 follows an $\alpha(\lambda)$ relation [20] given by

$$\alpha(\lambda) = \frac{(\beta - 1)}{[(1 + r_2/\lambda)e^{-r_2/\lambda} - \beta(1 + r_1/\lambda)e^{-r_1/\lambda}]}. \qquad (13)$$

Varying β within the limits of experimental uncertainties upper limits for the strength of a composition-independent fifth force can be obtained. Below 5 cm, where Eq. (13) is not exactly valid any more depending on the model used for the Luther experiment, and above 100 m, the typical mass separation in the Gigerwald experiment, the sensitivity to the fifth force strongly decreases. In the range between, however, we obtain new constraints for the strength of an attractive ($\alpha > 0$) and repulsive fifth force ($\alpha < 0$), respectively. They are shown in Fig. 15 together with other G experiments at geophysical distances.

ACKNOWLEDGMENTS

We thank W. Grünenfelder of the Kraftwerke Sarganserland KSL and Ch. Venzin of the Nordostschweizerische Kraftwerke NOK for the hospitality in the Gigerwald dam and helpful technical support. We would like to thank M. Baumeler of Mettler-Toledo AG in Greifensee, Switzerland, for providing the mass comparator and for the crucial collaboration to enhance its performance. We are indebted to Auer+Clement AG for air photogrammetry and to the Ingenieur-Büro Schneider for survey data. We gratefully acknowledge important contributions from A. Geiger, T. Kersten, and E. Klingele of the Institut für Geodäsie und Photogrammetrie der ETH Zürich and from H. Stüssi and J. Schurr of the Physik-Institut der Universität Zürich. This work was supported by the Schweizerische Nationalfonds and the Dr. Tomalla-Stiftung.

[1] For an index of theories and measurements, see E. Fischbach *et al.*, Metrologia **29**, 213 (1992); for a review, see F. D. Stacey *et al.*, Rev. Mod. Phys. **59**, 157 (1987); E. G. Adelberger *et al.*, Annu. Rev. Nucl. Part. Sci. **41**, 269 (1991); Y. Fujii, Int. J. Mod. Phys. A **6**, 3505 (1991); E. Fischbach and C. Talmadge, Nature (London) **356**, 207 (1992).

[2] E. G. Adelberger *et al.*, Phys. Rev. D **42**, 3267 (1990).

[3] C. Talmadge *et al.*, Phys. Rev. Lett. **61**, 1159 (1988).

[4] R. H. Rapp, Geophys. Res. Lett. **14**, 730 (1987).

[5] Y. T. Chen *et al.*, Proc. R. Soc. London **A394**, 47 (1984); J. K. Hoskins *et al.*, Phys. Rev. D **32**, 3084 (1985); V. P. Mitrofanov and O. I. Ponomareva, Zh. Eksp. Teor. Fiz. **94**, 16 (1988) [Sov. Phys. JETP **67**, 1963 (1988)].

[6] M. V. Moody and H. J. Paik, Phys. Rev. Lett. **70**, 1195 (1993).
[7] J. Schurr, Ph.D. thesis, Gesamthochschule Wuppertal, 1992.
[8] D. H. Eckhardt *et al.*, Phys. Rev. Lett. **60**, 2567 (1988); J. Thomas *et al.*, *ibid.* **63**, 1902 (1989); C. Jekeli *et al.*, *ibid.* **64**, 1204 (1990); C. C. Speake *et al.*, *ibid.* **65**, 1967 (1990); Y.-C. Liu *et al.*, Phys. Lett. A **169**, 131 (1992); A. J. Romaides *et al.*, Phys. Rev. D **50**, 3608 (1994).
[9] F. D. Stacey *et al.*, Phys. Rev. D **23**, 1683 (1981); S. C. Holding *et al.*, *ibid.* **33**, 3487 (1986).
[10] M. E. Ander *et al.*, Phys. Rev. Lett. **62**, 985 (1989).
[11] M. A. Zumberge *et al.*, Phys. Rev. Lett. **67**, 3051 (1991).
[12] G. Müller *et al.*, Phys. Rev. Lett. **63**, 2621 (1989); Geophys. J. Int. **101**, 329 (1990).
[13] M. Oldham *et al.*, Geophys. J. Int. **113**, 83 (1993).
[14] G. I. Moore *et al.*, Phys. Rev. D **38**, 1023 (1988); J. Phys. E **21**, 534 (1988).
[15] A. Cornaz, B. Hubler, and W. Kündig, Phys. Rev. Lett. **72**, 1152 (1994).
[16] Ingenieur-Büro Schneider AG, Chur.
[17] Measurement by E. Klingele, ETH Zürich.
[18] M. Talwani and M. Ewing, Geophysics **25**, 203 (1960).
[19] G. G. Luther and W. R. Towler, Phys. Rev. Lett. **48**, 121 (1982).
[20] G. W. Gibbons and B. F. Whiting, Nature (London) **291**, 636 (1981).